

High-Energy Photoprotons from Light Nuclei*

Y. S. KIM,[†] F. F. LIU,[‡] F. J. LOEFFLER, AND T. R. PALFREY, JR.

Department of Physics, Purdue University, Lafayette, Indiana

(Received 13 June 1962)

Photoprotons produced in Li, Be, B, and C targets by bremsstrahlung with a peak energy of 335 MeV were observed at eight angles between 20° and 96° in the laboratory. Protons with energies between 140 MeV and 192 MeV were detected by means of a scintillation counter telescope which simultaneously observed three adjacent energy bins. Corrections to the data for nuclear absorption in the target, multiple scattering in the target and counter telescope, pion contamination, and other small effects have been made. The results are compared with Levinger's quasi-deuteron model.

The width of the momentum distribution for the quasi-deuteron inside the nucleus and the differential cross section for the photodisintegration of the quasi-deuteron were used alternatively as adjustable quantities in fitting the data. If experimental data for the free deuteron photoeffect are used, it is found that a fairly wide momentum distribution with tails falling more slowly than those of a Gaussian is required for agreement with this measurement.

I. INTRODUCTION

THE photoproduction of protons from nuclei by high-energy bremsstrahlung has been observed and discussed in considerable detail.¹ At the present time the qualitative features of the process are fairly well understood and lead to the following conclusions:

(1) For the most part the photon is absorbed by a quasi-deuteron subunit in the nucleus.²

(2) Below meson threshold the process involves a quasi-deuteron with proton and neutron in a relative *S* state to give the proton the required high momentum. At higher photon energies the absorption may be with a "larger" deuteron since the emission and reabsorption of a pion in the quasi-deuteron can now account for the high observed momenta of the photoprotons. However, the lower initial angular momentum states of the quasi-deuteron would still seem to be favored since the meson re-absorption probability will be larger if the two nucleons are close together.

(3) The effect of the remaining *A* - 2 nucleons of the nucleus is to provide a potential well in which the quasi-deuteron resides and to scatter some of the outgoing high-energy nucleons (in the neighborhood of 30% for Li).¹ The motion of the quasi-deuteron in the well causes the kinematics of the photodisintegration process to be smeared out.

The present additional work was done primarily for practical reasons and also because of the stimulation of Cence and Moyer.³ In the course of measuring the polarization of photoprotons from light elements with a

counter polarimeter,⁴ it became apparent that we would need to determine the differential production cross section for photoprotons with greater accuracy than that with which it was currently known. This is because an artificial left-right asymmetry is introduced into a counter polarimeter measurement by a nonisotropic angular distribution. It was feasible to do this in a reasonable length of time because of the recently increased synchrotron beam intensity⁵ and so measurements were made at eight angles between 20° and 96° in the laboratory and at three proton energies between 140 and 192 MeV, for each of the four targets, Li, Be, B, and C. The peak energy of the bremsstrahlung spectrum was 335 MeV throughout the measurement.

Within the framework of a quasi-deuteron model for the photoabsorption process the experimental observations can be analyzed in essentially two different ways. One can assume the quasi-deuteron will have a differential cross section for photodisintegration which is essentially the same as that for a free deuteron and treat as a fitting parameter the width of the momentum distribution function that describes the motion of the quasi-deuteron inside the nucleus. Alternatively, one can choose a value for the momentum distribution width that is indicated by other experiments^{1,6} and then deduce the required differential cross section for the quasi-deuteron. We have investigated both approaches and present the results.

II. EXPERIMENTAL ARRANGEMENT

The source of photons used in the experiment was bremsstrahlung from the Purdue University Synchrotron with an internal target of 0.040-in.-diam Pt wire. The synchrotron was operated at the peak electron energy

* This work was supported in part both by the U. S. Atomic Energy Commission and through a Purdue Research Foundation XR research grant.

[†] This work constituted part of a thesis submitted by Y. S. Kim to the Purdue Graduate School in partial fulfillment of the requirements for the Ph.D. degree. Present address: Department of Physics, Ohio State University, Columbus, Ohio.

[‡] Present address: Stanford Linear Accelerator Center, Stanford University, Stanford, California.

¹ M. Q. Barton and J. H. Smith, *Phys. Rev.* **110**, 1143 (1958). This paper contains most of the references to preceding work.

² J. S. Levinger, *Phys. Rev.* **84**, 43 (1951).

³ R. J. Cence and B. J. Moyer, *Phys. Rev.* **122**, 1634 (1961).

⁴ F. F. Liu, F. J. Loeffler, T. R. Palfrey, Jr., and Y. S. Kim, *Phys. Rev.* **128**, 2784 (1962).

⁵ Purdue Synchrotron Annual Progress Report to the Atomic Energy Commission, 1961 (unpublished).

⁶ A. C. Odian, P. C. Stein, A. Wattenberg, B. T. Feld, and R. Weinstein, *Phys. Rev.* **102**, 837 (1956).

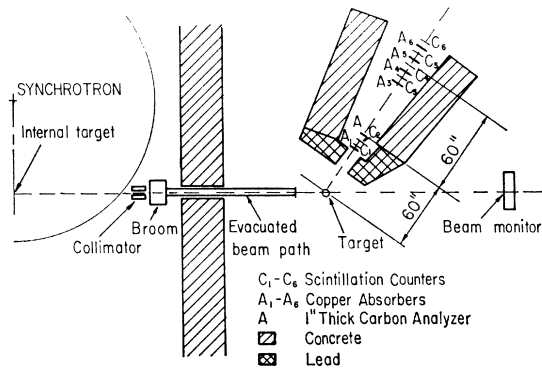


FIG. 1. Experimental setup.

of 335 MeV. The monitor used was a thick-walled ionization chamber of the Cornell type.⁷

The general experimental layout is shown in Fig. 1. The beam was collimated by a tapered lead collimator; the beam size at the position of the target was $1\frac{3}{4}$ in. high by $1\frac{1}{4}$ in. wide. The broom magnet following the collimator cleansed the beam of light charged particles. The beam then passed through an evacuated pipe which extended to within 14 in. of the target. The monitor was placed 60 in. from the target. A barite-loaded concrete wall, 20 in. thick, shielded the experimental area from the synchrotron.

The proton telescope used in this experiment was part of a scintillator counter polarimeter. This polarimeter was used in this laboratory for measuring the polarization of high-energy photoprotons.⁴ The carbon plate acted as an analyzer in the polarimeter; and the separation of the telescope into two parts was due to the mechanical construction of the polarimeter. The effective solid angle subtended by the telescope was 2.065×10^{-3} sr.

Conventional electronics were used. The two front counters were each viewed by RCA 6810-A photomultipliers. Signals from these counters were discriminated and put into a coincidence circuit of 50 nsec resolving time. Signals from back counters C3 through C6 were each fed into discriminators D3 through D6.

Photoprotons were counted in three energy bins. The first energy bin was defined by the requirement of a coincidence of C1, C2, and C3 with an antisignal from C4, this bin being denoted C1234. The other two energy bins were defined similarly. All discriminators were beam gated.

The method adopted in this experiment for proton identification and separation followed closely that of other investigators.^{8,9}

The front copper absorber A₁ eliminated all the low-energy electrons and all deuterons. Pion-proton separation

⁷ F. J. Loeffler, T. R. Palfrey, and G. W. Tauffest, Nucl. Instr. Methods **5**, 50 (1959).

⁸ J. C. Keck, Phys. Rev. **85**, 410 (1952).

⁹ B. T. Feld, R. D. Godbole, A. Odian, F. Scherb, P. C. Stein, and A. Wattenberg, Phys. Rev. **94**, 1000 (1954).

TABLE I. Differential cross sections.^a

θ_{lab}	Lithium		
	143 MeV	161 MeV	183 MeV
20°	0.310±0.010	0.189±0.007	0.102±0.006
30°	0.345±0.009	0.192±0.009	0.116±0.007
40°	0.296±0.009	0.167±0.007	0.103±0.005
51°	0.249±0.006	0.124±0.004	0.066±0.004
61°	0.214±0.006	0.091±0.004	0.045±0.003
74°	0.121±0.005	0.049±0.003	0.019±0.002
86°	0.081±0.004	0.028±0.002	0.006±0.001
96°	0.056±0.003	0.019±0.002	0.004±0.001
θ_{lab}	Beryllium		
	154 MeV	174 MeV	190 MeV
30°	0.280±0.010	0.181±0.008	0.145±0.007
40°	0.251±0.008	0.150±0.006	0.118±0.005
51°	0.185±0.005	0.085±0.003	0.062±0.003
61°	0.162±0.005	0.071±0.003	0.045±0.002
74°	0.132±0.004	0.049±0.002	0.028±0.001
86°	0.038±0.002	0.012±0.001	0.003±0.001
96°	0.030±0.002	0.009±0.001	0.002±0.001
θ_{lab}	Boron		
	140 MeV	160 MeV	179 MeV
20°	0.495±0.015	0.264±0.010	0.125±0.008
30°	0.503±0.013	0.276±0.009	0.180±0.008
40°	0.440±0.013	0.200±0.008	0.114±0.008
51°	0.397±0.011	0.160±0.006	0.087±0.006
61°	0.320±0.010	0.135±0.006	0.063±0.004
74°	0.190±0.006	0.085±0.004	0.038±0.003
86°	0.154±0.006	0.061±0.003	0.020±0.003
96°	0.118±0.006	0.036±0.001	0.006±0.001
θ_{lab}	Carbon		
	156 MeV	174 MeV	192 MeV
30°	0.462±0.010	0.234±0.007	0.154±0.006
40°	0.381±0.009	0.211±0.007	0.115±0.006
51°	0.334±0.004	0.142±0.003	0.085±0.003
61°	0.274±0.006	0.113±0.003	0.061±0.003
74°	0.136±0.003	0.052±0.002	0.027±0.002
86°	0.109±0.003	0.045±0.002	0.012±0.001
96°	0.075±0.003	0.026±0.002	0.008±0.001

^a In $\mu\text{b}/\text{sr}\cdot\text{MeV}$ per equivalent quantum.

tion in this experiment was made essentially in the front two counters. We need to consider only those pions and protons that have the same range in the back counter telescope. By constructing the Landau curves¹⁰ for the energy losses of pions and protons in the front counters, and knowing the production ratio of pions and protons, estimates showed that the pion contamination was negligible in this experiment at all angles and for all elements. Bias curves also indicated no meson contamination.

III. CORRECTIONS TO DATA

The principal experimental correction in this experiment was that for nuclear attenuation in the target and in the counter telescope. This correction was made in the manner of that used by Keck and Tollestrup.¹¹ These corrections varied from 18 to 36%, and are sub-

¹⁰ B. Rossi, *High Energy Particles* (Prentice-Hall, Inc., Englewood Cliffs, New Jersey, 1952), Chap. 2, p. 30.

¹¹ J. C. Keck and A. V. Tollestrup, Phys. Rev. **101**, 360 (1956).

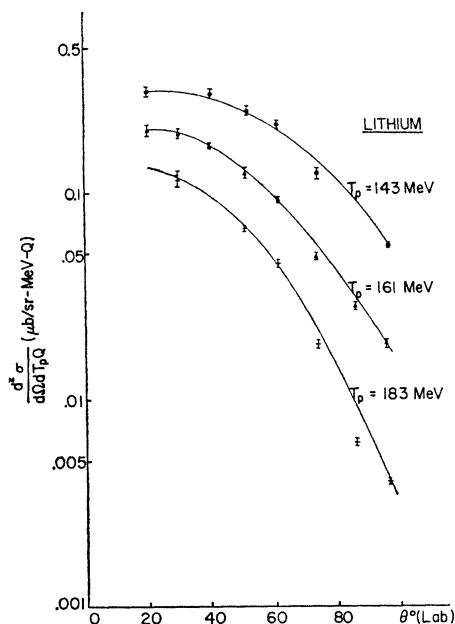


FIG. 2. Differential cross sections for photoproton production from lithium.

ject to an error of about 6%. Their influence on the reliability of the final experimental results is thus 1-2%.

The counter telescope was designed in such a way that multiple Coulomb scattering was expected to be negligible. Detailed computer calculations performed afterwards indicated that there was no correction needed for multiple scattering effects.

Because the targets used were rather thick, it was necessary to make corrections for the attenuation of the

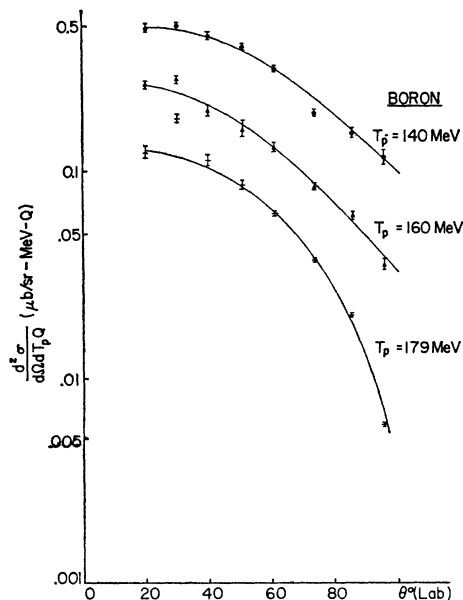


FIG. 3. Differential cross sections for photoproton production from beryllium.

gamma-ray beam in the target, and for the influence of the target on the response of the monitor. The latter correction was made experimentally by reference to a thin-walled, secondary ionization chamber placed well ahead of the target in the gamma-ray beam in a series of target-in, target-out runs. The former correction was then made on the basis of the known pair-production cross sections at the appropriate gamma-ray energies. The total correction from these two effects was 4% in carbon, and less in the other targets.

IV. EXPERIMENTAL RESULTS

The laboratory differential cross sections for photoproton production were calculated using the corrected data from the following equation:

$$d^2\sigma/d\Omega dT_P \text{ per equivalent quantum} = n/\Delta\Omega N_T \Delta T_P Q,$$

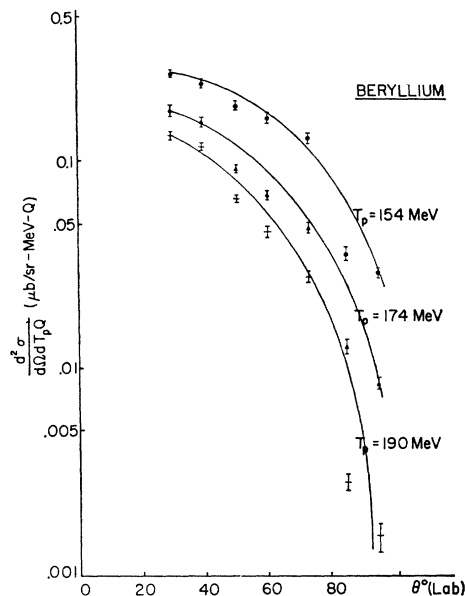


FIG. 4. Differential cross sections for photoproton production from boron.

where $\Delta\Omega$ is the detector solid angle, N_T is the number of target nuclei per cm^2 , n is the corrected counts obtained in Q equivalent quanta, and ΔT_P is the bin width in MeV. The results are shown in Table I and also are plotted in Figs. 2-5 for the various laboratory proton energies and targets studied. The errors shown are the statistical uncertainties only and do not show a probable error of 4% due to uncertainties of the target density, bin width, solid angle, effective quanta, etc.

The 30° differential cross sections divided by NZ/A are plotted against the atomic number Z in Fig. 6 for the three proton energies, 140, 160, and 179 MeV. Figure 7 shows the comparison of the experimental results from lithium with the Levinger model for two different momentum distributions.

V. DISCUSSION OF RESULTS

A Levinger-type calculation was made of the cross section for the production of high-energy protons from complex nuclei. Following Levinger¹² and Wilson,¹³ we assume that the initial-state wave function of the complex nuclei Ψ_Z' can be written as a product of three wave functions:

$$\Psi_Z' = \Phi_R(\mathbf{R}) Y_Z(\mathbf{r}) \phi(A-2), \quad (2)$$

where $\Phi_R(\mathbf{R})$ describes the center of mass of the quasi-deuteron, $Y_Z(\mathbf{r})$ is the quasi-deuteron wave function in the proton-neutron relative coordinates \mathbf{r} , and $\phi(A-2)$ represents the residual nucleon wave function. We assume with Levinger and Wilson that the cross section for the production of high-energy protons will depend only on the quasi-deuteron wave function $Y_Z(\mathbf{r})$. Now,

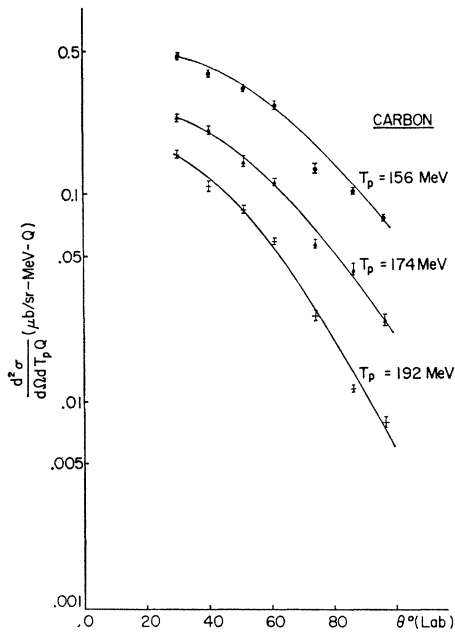


FIG. 5. Differential cross sections for photoproton production from carbon.

since the wave function of the two-nucleon system is not likely to depend heavily on the eigenenergy, E_b , of the system in the energy range concerned in this discussion (E_b is -2.226 MeV for the free deuteron and about 10 MeV for the quasi-deuterons),¹ we assume that $Y_Z(\mathbf{r})$ is related to the free deuteron wave function $\psi_D(\mathbf{r})$ by

$$Y_Z(\mathbf{r}) = \alpha^{1/2} \psi_D(\mathbf{r}), \quad (3)$$

where α represents the probability of having a neutron-proton pair so close as to participate in the absorption of a photon. Then, the quasi-deuteron photodissociation cross section σ_Z is related to the free deuteron dissociation

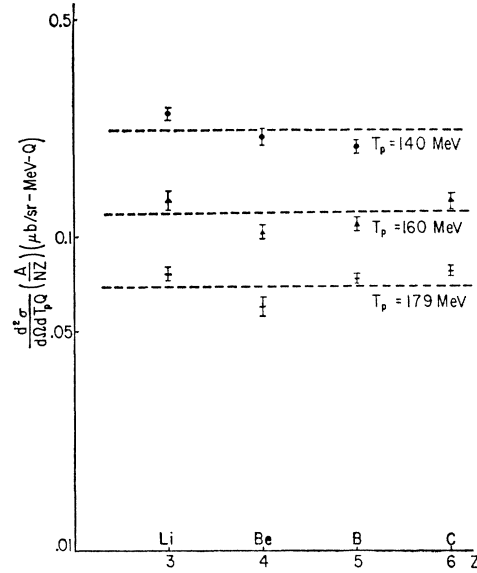


FIG. 6. Dependence of the photoproton differential cross section on atomic number Z at $\theta_{lab} = 30^\circ$.

cross section σ_D by

$$\sigma_Z = \alpha NZ \sigma_D. \quad (4)$$

NZ represents the probability of having a neutron-proton pair. If one writes $\alpha = L/A$, where A is the mass number, Eq. (4) takes the familiar form

$$\sigma_Z = L(NZ/A) \sigma_D. \quad (4a)$$

Assuming that the main effect of the motion of the center of mass of the quasi-deuteron is the smearing out of the kinematics, the differential cross section per

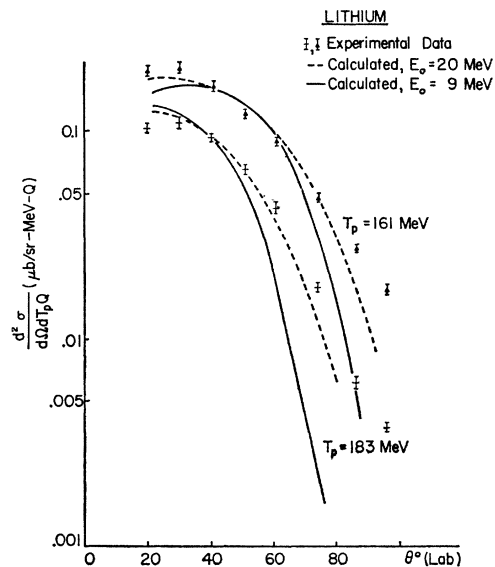


FIG. 7. Comparison of the experimental results from lithium with the Levinger model for two different internal momentum distributions.

¹² J. S. Levinger, Phys. Rev. **84**, 43 (1951).

¹³ R. R. Wilson, Phys. Rev. **104**, 218 (1956).

equivalent quantum can be written:

$$\frac{d^2\sigma}{d\Omega dT_P} = L \frac{NZ}{A} \int \int d\mathbf{p}_x d\mathbf{p}_y P(\mathbf{p}_x) P(\mathbf{p}_y) \times \frac{d\sigma}{d\Omega'} \frac{dk}{dT_{P'}} \frac{dT_{P'}}{dT_P} \frac{d\Omega'}{d\Omega} \frac{B(k_0, k)}{k}. \quad (5)$$

The primes refer to the coordinate system in which the center of mass of the quasi-deuteron is at rest. The momentum distribution functions $P(\mathbf{p}_x)$ and $P(\mathbf{p}_y)$ are assumed to be Gaussian, i.e.,

$$P(\mathbf{p}) = (4\pi E_0 M)^{-3/2} \exp[-\mathbf{p}^2 / (4E_0 M)], \quad (6)$$

where M is the nucleonic mass and E_0 is an adjustable parameter given in MeV. The other quantities appearing in Eq. (5) are: $T_{P'}$, the proton energy in the primed system; T_P , the proton energy in the laboratory; k , the photon energy in the laboratory; $B(k_0, k)$, the appropriately normalized Schiff bremsstrahlung function with peak energy k_0 ¹⁴; $d\sigma/d\Omega'$ the photodisintegration cross section of the quasi-deuteron in the primed system.

The double integral was numerically evaluated. An IBM 7090 digital computer was used for the computation. The calculated cross sections for Li are compared with the experimental data in Fig. 7. L was assumed to be 6.4, the value predicted by Levinger.¹² It was assumed that the photoprotons lost on the average about 15 MeV in escaping from the nucleus. The agreement is quite good for $E_0 = 20$ MeV but only fair for $E_0 = 9$ MeV. The poor agreement at large angles is expected from the scattering of the photoprotons by the residual nucleons. Low values of E_0 fail to account for the rather large number of protons at large angles to the gamma ray beam. One cannot say from the results of this experiment whether this discrepancy is due to nuclear scattering of the outgoing nucleon in the parent nucleus, or perhaps due to the breakup of quasi-alpha particles in the original interaction. In any event, these effects are sufficiently large to permit the fitting of a wide variety of internal momentum distributions to the data, and to encourage the choice of a larger value of the Gaussian parameter E_0 than that suggested by the experiments of Barton and Smith¹ or Feld *et al.*⁹ The results of this experiment agree with previous experiments in that the photoproton cross section is observed to be proportional to NZ/A over the entire angular and energy region examined, a result consistent with a quasi-deuteron model.

One may assume from the experiments of Barton and Smith,¹ of Feld *et al.*,⁹ and of Cence and Moyer,³ that our knowledge of the internal momentum distribution of the quasi-deuteron is not bad. On this basis, one can attempt to estimate the quasi-deuteron photodisintegration cross section $d\sigma/d\Omega$ plus the scattering effects from our

TABLE II. The values of coefficients in the differential cross section $d\sigma/d\Omega$.

T_P (MeV)	A	B	C	D
161	+3.1	-15.7	+42.3	-26.4
182	+0.4	+2.5	-9.4	+7.3

experimental cross sections. We assume that $d\sigma/d\Omega$ is fairly independent of energy, and that E_0 is 9 MeV. The disagreement between the calculated and the measured cross sections are then assumed to be due to the difference between the free deuteron dissociation cross section and the quasi-deuteron cross section and the scattering effects. In these calculations $d\sigma/d\Omega$ is assumed to have the following form:

$$d\sigma/d\Omega = A + B \cos\theta + C \cos^2\theta + D \cos^3\theta,$$

where θ is the center-of-mass angle of the photon in the quasi-deuteron system. This form was put into Eq. (5) in place of $d\sigma/d\Omega'$ with a solid angle conversion factor and the integral was evaluated. These integrals were used as fitting functions and the coefficients A , B , C , and D were calculated from the experimental values of the cross section. The coefficients are listed in Table II. These values have a probable error of 30%. It is obvious that this method of calculation does not give a consistent result. In the first place, it is extremely sensitive to the high angle data. In the second place, both sets of numbers give unphysical results for angles beyond the measured region—in particular at 180°. The principal conclusion to be drawn from this method of handling the data is that the effects which modify agreement with the usual method of fitting by choice of a quasi-deuteron internal momentum distribution are magnified by this approach, and effectively prevent a comparison of the cross sections for the photodisintegration of real and of quasi-deuterons.

Any direct comparison of the absolute differential cross sections with other experiments is very difficult. This is because none of the existing photoproton data cover exactly the same energies and angles as this experiment and making interpolations introduces significant errors because of the sharp energy and angular

TABLE III. Comparison to other experiments.

Author	T_P (MeV)	θ	Cross section
Keck ^a	175	67.5°	0.086 ± 0.008
This exp't.	174	61°	0.107 ± 0.003
Feld ^b	126	30°	0.45 ± 0.14
This exp't.	156	30°	0.46 ± 0.01
Rosengren ^c	170	90°	0.11 ± 0.05
This exp't.	176	86°	0.044 ± 0.002

^a See reference 8.

^b See reference 9.

^c J. W. Rosengren and J. M. Dudley, Phys. Rev. **89**, 603 (1953).

¹⁴ L. I. Schiff, Phys. Rev. **70**, 87 (1946).

dependence of the cross sections. However, an order-of-magnitude comparison is made here to check the consistency of the carbon data of this experiment with that of other experiments. Table III gives a comparison to some of the previous data. The units of the cross section are $\mu\text{b}/\text{sr}\cdot\text{MeV}$ per equivalent quantum.

The linear dependence of the cross sections on ZN/A as seen in Fig. 6 is in agreement with other experiments.^{6,8,9}

Future experiments should look carefully into the effect, if any, of alpha-particle substructures in the nucleus on the angular distribution of photoprotons. Furthermore, as Cence and Moyer have suggested, future experiments should either be done with photon-

beam monochromators, or with photon-difference techniques. Either of these techniques would permit a reasonable separation of the effect of scattering in the parent nucleus from other effects.

ACKNOWLEDGMENTS

The authors wish to acknowledge the help and support of the synchrotron staff during the course of this experiment.

We are particularly indebted to Gene Durr who built many of the electronics circuits, to Donald Banes who operated the synchrotron for a good part of the running time, and to Dr. R. O. Haxby for several consultations during the runs.

Hyperons with and without Doublet Symmetry. II*

GREGOR WENTZEL

*Enrico Fermi Institute for Nuclear Studies and Department of Physics,
University of Chicago, Chicago, Illinois*

(Received 26 July 1962)

Earlier work on hyperon isobars (resonances) based on a static strong-coupling approximation is continued. New results are derived, in particular for values near ± 1 and near 0 of the ratio of the two coupling constants ($\Sigma\Sigma\pi$ to $\Lambda\Sigma\pi$).

The orbital angular momentum l of a stationary (or resonant) state is unambiguously defined through the eigenfunctions of the bound-pion Hamiltonian. For instance a resonance with $l=2$ and isospin 0 is predicted if the direct $\Sigma\Sigma\pi$ coupling is very weak or absent.

1. INTRODUCTION

A STRONG-COUPLING treatment of hyperon-pion interactions, with emphasis on bound states or resonances, was carried through, with some limitations, in an earlier paper under the same title.¹ Additional results on the same topic are reported here.

The interaction Hamiltonian to be studied is

$$H_1 = g(\Lambda^\dagger \sigma \Sigma + \Sigma^\dagger \sigma \Lambda) \cdot \nabla \Psi_{\text{av}} + g' i(\Sigma^\dagger \times \sigma \Sigma) \cdot \nabla \Psi_{\text{av}}. \quad (1)$$

In I, the corresponding scalar interaction ($\sigma \cdot \nabla \rightarrow 1$) was treated for an arbitrary ratio ($\alpha = g'/g$) of the two independent coupling constants. The more interesting, but more difficult, pseudoscalar interaction (1) was explored only for the special case $g'=0$ (I, Appendix), while the results are well known for $g' = \pm g$ by virtue of doublet (or global) symmetry. Generalizations of these special results are our concern here.

For reference, previous findings have been summarized in Table I. Excitation energies, in arbitrary units, are listed in the third and fourth columns for the two special cases. While these energy differences become continuous functions of the coupling constants g, g' ,

* This work was supported by the United States Atomic Energy Commission.

¹ G. Wentzel, Phys. Rev. **125**, 771 (1962), to be quoted as I.

the quantum numbers assigned to the various states, as listed in the second column, are adiabatic invariants (although not obvious, this turns out to be true even for l). Hence, these quantum numbers retain their significance if the coupling strengths are scaled down to more realistic values (intermediate coupling). This provides a kind of information which is not so easily accessible to the more popular methods of analysis,² concerned primarily with the S matrix. Instead, we study the Schrödinger equation of the problem; we can explicitly construct the eigenfunctions of "stationary" states and by inspection determine their quantum numbers. For instance, if the state " Y_0^* " is called a d state, this has the precise meaning that its eigenfunctions are linear combinations (corresponding to $j = \frac{3}{2}$) of the five spherical harmonics $l=2$ (see I, p. 776).³ The physical Σ appears as a $p_{1/2}$ state. Of course, all states have the same parity.

² D. Amati, A. Stanghellini, and B. Vitale, Nuovo Cimento **13**, 1143 (1959); Phys. Rev. Letters **5**, 524 (1960); M. Nauenberg, *ibid.* **2**, 351 (1959); J. Franklin, R. C. King, and S. F. Tuan, Phys. Rev. **124**, 1995 (1961); T. L. Trueman, *ibid.* **127**, 2240 (1962).

³ Note, however, that these are the (one-component) eigenfunctions of the transformed Hamiltonian $U^\dagger H U$.